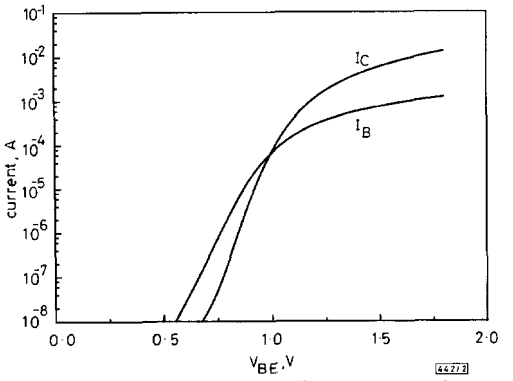

Fig. 2 *Gummel plot of pseudomorphic AlInP/InP HBT with emitter area of 40×40μm²*

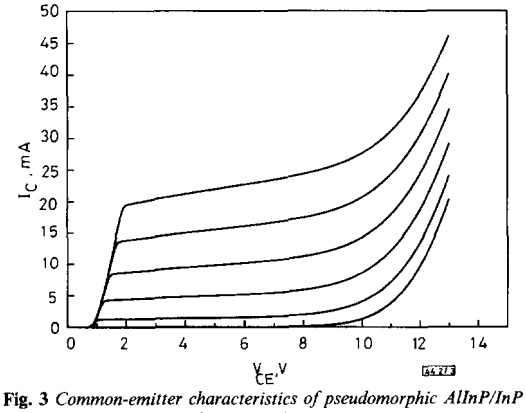

Fig. 3 *Common-emitter characteristics of pseudomorphic AlInP/InP HBT with emitter area of 40×40μm²*

I_B step = 250μA

Gummel plot is shown in Fig. 2. Ideality factors for base and collector current were 1.7 and 1.3, respectively. We estimate that the 15% Al composition results in a bandgap difference between emitter and base of 87 meV (after accounting for strain effects). The common-emitter I/V characteristics are shown in Fig. 3. The common-emitter breakdown voltage BV_{CEO} was of the order of 10 V, while the common-base breakdown voltage BV_{CBO} was 13V. BV_{CBO} is not much larger than BV_{CEO}, and both values are somewhat smaller than estimated values for ideal InP *p-n* junctions. The breakdown voltages can most likely be attributed to surface breakdown as opposed to junction breakdown. Nonetheless this is a significant improvement over devices with an InGaAs base and collector.

Summary: We have presented novel HBTs with pseudomorphic wide-bandgap AlInP emitters and InP base and collector regions. The devices permit the use of InP collectors in a way that avoids a conduction-band barrier between base and collector. These devices are candidates for high speed and/or high breakdown HBT applications.

23 November 1994
Electronics Letters Online No: 19950084

Y.M. Hsin, M.C. Ho, X.B. Mei, H.H. Liao, T.P. Chin, C.W. Tu and P.M. Asbeck (*Department of Electric and Computer Engineering, University of California, San Diego, La Jolla, CA 92093-0407, USA*)

References

1 NOTTENBURG, R.N., CHEN, Y.K., PANISH, M.B., HAMM, R., and HUMPHREY, D.A.: 'High-current-gain submicrometer InGaAs/InP heterostructure bipolar transistors', *IEEE Electron. Device Lett.*, 1988, **9**, pp. 524–526

2 CHEN, Y.K., NOTTENBURG, R.N., PANISH, M.B., HAMM, R., and HUMPHREY, D.A.: 'Subpicosecond InP/InGaAs heterostructure bipolar transistors', *IEEE Electron. Device Lett.*, 1989, **10**, pp. 267–269

3 CHAU, H.F., and BEAM, E.A.: 'High-speed InP/InGaAs heterojunction bipolar transistors', *IEEE Electron. Device Lett.*, 1993, **14**, (8), pp. 388–390

4 SONG, J.I., HONG, B.W.P., PALMSTROM, C.J., VAN DER GAAG, B.P., and CHOUGH, K.B.: 'Ultra-high-speed InP/InGaAs heterojunction bipolar transistors', *IEEE Electron. Device Lett.*, 1994, **3**, p. 94

5 TOKUMITSU, E., DENTAI, A.G., JOYNER, C.H., and CHANDRASEKHAR, S.: 'InP/InGaAs double heterojunction bipolar transistors grown by metalorganic vapor phase epitaxy with sulfur delta doping in the collector region', *Appl. Phys. Lett.*, 1990, **57**, (26), pp. 2841–2843

6 FEYGENSON, A., HAMM, R.A., SMITH, P.R., PINTO, M.R., MONTGOMERY, R.K., YADVISH, R.D., and TEMKIN, H.: 'A 144GHz InP/InGaAs composite collector heterostructure bipolar transistor'. IEDM 92-75, 1992, pp. 75–78

7 CHAU, , PAVLIDIS, D., HU, J., and TOMIZAWA, K.: 'Breakdown-speed considerations in InP/InGaAs single- and double-heterostructure bipolar transistors', *IEEE Trans.*, 1993, **ED-40**, (1), pp. 2–8

8 KURISHIMA, K., NAKAJIMA, H., KOBAYASHI, T., MATSUOKA, Y., and ISHIBASHI, T.: 'Fabrication and characterization of high-performance InP/InGaAs double-heterojunction bipolar transistors', *IEEE Trans.*, 1994, **ED-41**, (8), pp. 1319–1326

9 LIN, K.C., HSIN, Y.M., CHANG, C.Y., and CHANG, E.Y.: 'A pseudomorphic GaInP/InP MESFET with improved device performance', *IEEE Trans.*, 1993, **ED-40**, (12), pp. 2361–2362

Adaptive VS-MRAC for disturbance cancellation

E. Bertran and G. Montoro Lopez

Indexing terms: Model reference adaptive control system, Interference suppression

A variable structure, model reference adaptive control (VS-MRAC) devoted to cancel interferences without the requirement of an auxiliary input is proposed. This method is an improved alternative to the strategies recently proposed in the control theory literature.

Introduction: In the general structure of a conventional noise canceller [1], the reference signal, which must be correlated with the additive noise, can be obtained from the measurement of the interference at some point of the system. When that is not possible due either to the impossibility of observing or measuring the interference noise, the conventional canceller structure is not useful.

Non-adaptive VS-MRAC controllers can cancel interferences or unmodelled dynamics with only the requirement of the prior information concerning the interference bounds [2]. These methods show a fast response with zero error, but present chattering problems due to the switching functions that appear in the control law. Adaptive VS-MRAC controllers are used when the interference bound is unknown: the bound is obtained adaptively [3, 4]. Recently [4], a new method has been proposed that uses an integral law to generate the adaptive bound, with a zero output tracking error, in spite of chattering phenomena.

We propose a proportional-integral based law to generate the adaptive bound. This method reduces chattering and high frequency harmonics, assuring that the error tends to zero.

VS-MRAC canceller: The system (ARMAX) describing the evolution of the error is represented by the state equations [5]

$$\begin{aligned}\dot{x}(t) &= Ax(t) + bv(t)\\ \varepsilon(t) &= c^T x(t) = y_p(t) - y_m(t)\\ v(t) &= u(t) - \varphi^T(t)\alpha + i_f(t)\\ u(t) &= \varphi^T(t)k(t) + u_i(t)\end{aligned} \tag{1}$$

where $i_f(t)$ is the interference to cancel, referred to the input. The plant output is $y_p(t)$, $y_m(t)$ the model output, and $u(t)$ the control signal. The transfer function $H(s)$ between $\varepsilon(t)$ and $v(t)$ is

$$H(s) = c^T(sI - A)^{-1}b \tag{2}$$

and must be an SPR (strictly positive real function) function [5]. Therefore, defining the vector $\phi(t) = k(t) - \alpha$, the error equations can be rewritten as

$$\begin{aligned}\dot{x}(t) &= Ax(t) + bv(t)\\ \varepsilon(t) &= c^T x(t)\\ v(t) &= \varphi^T(t)(k(t) - \alpha) + u_i(t) + i_f(t)\\ &= \varphi^T(t)\phi(t) + u_i(t) + i_f(t)\end{aligned} \tag{3}$$

The $k(t)$ vector is selected according to an integral law: it is a classical adaptive algorithm if the plant is disturbance free. The $u_i(t)$ signal, devoted to cancel the interference, is chosen as in [2, 6]

$$\begin{aligned}\dot{k}(t) &= \dot{\phi}(t) = -R\varphi(t)\varepsilon(t)\\ u_i(t) &= -\mathrm{sgn}(\varepsilon)\max(|i_f|)\end{aligned} \tag{4}$$

where $\max(|i_f|)$ is a bound for $|i_f|$. The Lyapunov function candidate is

$$L = x^T(t)Px(t) + \phi^T(t)R^{-1}\phi(t) \tag{5}$$

where P is a positive definite matrix, and R is a positive definite diagonal matrix. The time derivative of L is given by

$$\begin{aligned}&\dot{L} = -x^T(t)Qx(t) + 2\varepsilon(t)(-\mathrm{sgn}(\varepsilon)\max(|i_f|) + i_f(t)) \le 0\\ &\dot{L} \le -x^T(t)Qx(t) \Rightarrow \lim_{t\to\infty}\int_0^t x^T(\tau)Qx(\tau)d\tau \le L(0)\end{aligned} \tag{6}$$

where Q is a positive definite matrix [5]. Hence L is bounded and converges to a finite value. Moreover, $x(t)$ is continuous due to its derivative being bounded. Therefore, it follows from the Barbalat lemma that $x(t) \to 0$ when $t \to \infty$ [5].

Adaptive VS-MRAC canceller: If the bound of $i_f(t)$ is unknown then it can be obtained adaptively [3, 4]. We propose a new solution: the adaptive generation of the unknown bound with an integral-proportional based law. The $u_i(t)$ signal is

$$\begin{aligned}&u_i(t) = -\mathrm{sgn}(\varepsilon)M(t)\\ &\dot{M}(t) = \mu_1|\varepsilon(t)| + \mu_2|\dot{\varepsilon}(t)| \Rightarrow \frac{\dot{M}(t) - \mu_2|\dot{\varepsilon}(t)|}{\mu_1} = |\varepsilon(t)|\end{aligned} \tag{7}$$

with $\mu_i > 0$. We can consider a zero initial condition for $M(t)$. A Lyapunov function candidate is

$$\begin{aligned}L &= x^T(t)Px(t)\\ &+ \phi^T(t)R^{-1}\phi(t) + \frac{(M(t) - \max(|i_f|) - \mu_2|\varepsilon(t)|)^2}{\mu_1}\end{aligned} \tag{8}$$

The time derivative of L is given by

$$\begin{aligned}\dot{L} &= -x^T(t)Qx(t) + 2\varepsilon(t)(-\mathrm{sgn}(\varepsilon)\max(|i_f|)\\ &\quad + i_f(t)) - 2\mu_2|\varepsilon(t)|^2 \le 0\\ \dot{L} &\le -x^T(t)Qx(t)\end{aligned} \tag{9}$$

as in eqn. 6, it follows that $x(t) \to 0$ and $\varepsilon(t) \to 0$ when $t \to \infty$. The choice of $\mu_2 = 0$, leads to an integral law, like in [4].

Simulation results: The plant, reference model and error equations are defined by

$$\begin{aligned}\dot{x}_p(t) &= -b_p x_p(t) + a_p u(t)\\ \dot{x}_m(t) &= -b_m x_m(t) + a_m u_c(t)\\ y_p(t) &= x_p(t) + i(t)\\ y_m(t) &= x_m(t)\\ \dot{\varepsilon}(t) &= -b_m\varepsilon(t)\\ &\quad + a_p\left(u(t) - \frac{b_p - b_m}{a_p}y_p(t) - \frac{a_m}{a_p}u_c(t) + i_f(t)\right)\end{aligned} \tag{10}$$

where $\varepsilon(t) = y_p(t) - y_m(t)$. Therefore $u(t)$ and $H(s)$ are

$$\begin{aligned}&u(t) = K_1(t)y_p(t) + K_2(t)u_c(t) + u_i(t)\\ &H(s) = \frac{a_p}{s + b_m} \quad a_p > 0 \quad a_m > 0\end{aligned} \tag{11}$$

$H(s)$ is SPR. The k_i parameters are generated from

$$\begin{aligned}\dot{K}_1(t) &= -\gamma_1\varepsilon(t)y_p(t)\\ \dot{K}_2(t) &= -\gamma_2\varepsilon(t)u_c(t)\end{aligned} \tag{12}$$

where $\gamma_i > 0$. The signal $u_i(t)$ is given by

$$\begin{aligned}&u_i(t) = -\mathrm{sgn}(\varepsilon)M(t)\\ &VS\text{-}MRAC : M(t) = M = \max(|i_f|)\\ &adaptive\ VS\text{-}MRAC : M(t) = \mu_1\int_0^t|\varepsilon(\tau)|d\tau + \mu_2|\varepsilon(t)|\end{aligned} \tag{13}$$

The previous systems have been simulated with the parameters $a_m = 1$, $b_m = 1$, $a_p = 0.9$, $b_p = 1.2$, $\gamma_1 = \gamma_2 = 1$. The command signal $u_c(t)$ is a square wave and $i(t)$ is a strong interference defined by $i(t) = \sin(0.5t) + \sin(t) + \sin(2t) + \sin(3t)$.

The SIMNON graphic results (see Figs. 1 and 2) are:

a Proposed adaptive VS-MRAC: $\mu_1 = 1$, $\mu_2 = 50$

b Adaptive VS-MRAC: $\mu_1 = 1$ (integral law)

c VS-MRAC: $\max(|i_f|) = 6$

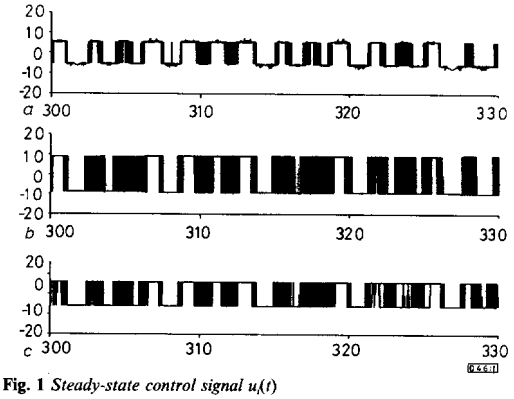

Fig. 1 *Steady-state control signal $u_i(t)$*

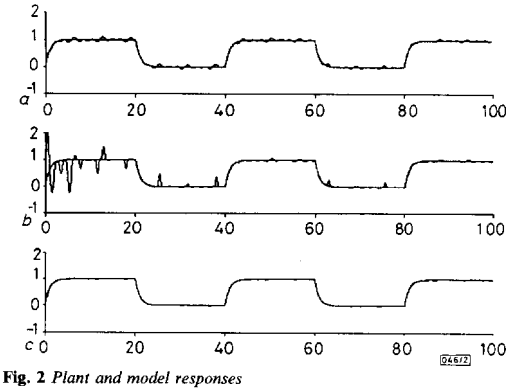

Fig. 2 *Plant and model responses*

Conclusions: The simulation results show the good behaviour of the proposed adaptive system, even for strong interferences in the same spectral band of the plant. In spite of the use of the signum function, the control signal $u_1(t)$ shows a lower chattering content (high frequencies) than the equivalent signal proposed in previous works. Apart from hardware considerations, this aspect has a significant importance in telecommunication applications. The method has been studied with other types of perturbations, unmodelled dynamics and nonlinearities in the plant, with similar results as above.

21 October 1994

Electronics Letters Online No: 19950088

E. Bertran and G. Montoro López (*Department of Signal Theory and Communications, Universitat Politecnica de Catalunya, PO Box 30.002, 08080 Barcelona, Spain*)

References

1 COWAN, C.F.W., and GRANT, P.M. (Eds.): 'Adaptive filters' (Prentice-Hall, 1985)

2 HSU, L.: 'Variable structure model-reference adaptive control (VS-MRAC) using only input and output measurements: Part II'. Proc. 27th IEEE Conf. Decision and Control, December 1988, pp. 2396–2401

3 NARENDRA, K.S., and BOSKOVIC, J.D.: 'A combined direct, indirect and variable structure method for robust adaptive control'. Proc. Automatic Control Conf., May 1990, pp. 543–548

4 FENG, G.: 'New robust model reference adaptive control algorithm', *IEE Proc. Control Theory Appl.*, May 1994, **141**, pp. 177–180

5 NARENDRA, K.S., and ANNASWAMY, A.M.: 'Stable adaptive systems' (Prentice-Hall, 1989)

6 BERTRAN, E., and MONTORO, G.: 'Application of hyperstability theory to interference cancelling'. Proc. 7th Mediterranean Electrotechnical Conf., April 1994, Vol. 2, pp. 679–682

ERRATA

LING, C.H., AH, L.K., and YEOW, Y.T.: 'Observation of current spikes in thin oxide MOS capacitor', *Electron. Lett.*, 1994, **30**, (24), pp. 2077–2079

Printers corrections

In the subcaption to Fig. 1, '815' should read '815000'
In the subcaption to Fig. 2, '30mW' should read '30mV'
In the line below Fig. 2, 'scaned' should read 'scanned'
In the caption to Fig. 3, 'Cuurent' should read 'Current'

Authors' correction

In the subcaptions to Fig. 3, the first line should read 'Hold time [s] at $V_g = 2$V:'

Editor's corrections

In the subcaptions to Fig. 3, '*a*' to '*h*' should read '(i)' to '(viii)'

In line 11 on p. 2079, and on the right-hand side of Fig. 4, the minus sign should read '≃'

SHIEH, J.-L., CHYI, J.-I., LIN, R.-J., LIN, R.-M., and PAN, J.-W.: 'Band offsets of $In_{0.30}Ga_{0.70}As/In_{0.29}Al_{0.71}As$ heterojunction grown on GaAs substrate' *Electron. Lett.*, 1994, **30**, (25), pp. 2172–2173

Authors' correction

In Table 1, the entries for 'Charge neutrality level' should read '0.39' and '0.68' respectively19th January 1995

ESTIMATION OF LENGTH FOR *ELECTRONICS LETTERS* VERSION 4.0

Title	1 column cm per 80 characters
Indexing terms	1.5 column cm (this includes adjacent space)
Abstract	1 column cm per 165 characters
Authors	1 column cm, plus 1 column cm for each address
Text	1 column cm per 165 characters (it is easiest to estimate the number of characters, including spaces, per line and the number of lines per page); add 0.5 or even 1 column cm for each equation or line in a matrix unless it is well displayed; counts of words or even characters made by word processors are not reliable for this purpose
References	1 column cm each
Tables	1 to 2 column cm for the title, 0.4 column cm for each line, including blanks; wide tables will be reshaped by editorial staff and the estimate adjusted accordingly
Figure captions	1 column cm for the main caption, 0.33 column cm per line for subcaptions, including keys which would be moved from the graphics
Figures	These are usually reduced to single column width (8.6 cm) at constant ratio of height to width; if the Figure is illegible at this reduction, the editing staff will redraw it and the height will be recalculated accordingly